

Noise-assisted spike propagation in myelinated neurons

Anna Ochab-Marcinek, Gerhard Schmid, Igor Goychuk, Peter Hänggi

Angaben zur Veröffentlichung / Publication details:

Ochab-Marcinek, Anna, Gerhard Schmid, Igor Goychuk, and Peter Hänggi. 2009. "Noise-assisted spike propagation in myelinated neurons." *Physical Review E* 79 (1): 011904. <https://doi.org/10.1103/physreve.79.011904>.

Nutzungsbedingungen / Terms of use:

licgercopyright

Dieses Dokument wird unter folgenden Bedingungen zur Verfügung gestellt: / This document is made available under these conditions:

Deutsches Urheberrecht

Weitere Informationen finden Sie unter: / For more information see:

<https://www.uni-augsburg.de/de/organisation/bibliothek/publizieren-zitieren-archivieren/publiz/>



Noise-assisted spike propagation in myelinated neurons

Anna Ochab-Marcinek,^{1,2} Gerhard Schmid,¹ Igor Goychuk,¹ and Peter Hänggi¹

¹*Institut für Physik, Universität Augsburg, Universitätsstraße 1, 86159 Augsburg, Germany*

²*M. Smoluchowski Institute of Physics, Jagellonian University, ul. Reymonta 4, 30-059 Kraków, Poland*

(Received 23 September 2008; published 9 January 2009)

We consider noise-assisted spike propagation in myelinated axons within a multicompartiment stochastic Hodgkin-Huxley model. The noise originates from a finite number of ion channels in each node of Ranvier. For the subthreshold internodal electric coupling, we show that (i) intrinsic noise removes the sharply defined threshold for spike propagation from node to node and (ii) there exists an optimum number of ion channels which allows for the most efficient signal propagation and it corresponds to the actual physiological values.

DOI: [10.1103/PhysRevE.79.011904](https://doi.org/10.1103/PhysRevE.79.011904)

PACS number(s): 87.18.Tt, 05.40.-a, 87.16.Xa, 87.19.lq

I. INTRODUCTION

In many vertebrates, the propagation of nerve impulses is mediated by myelinated axons. These nerve fibers are composed of active zones, the so-called nodes of Ranvier, where ion channels are accumulated, and passive fragments which are electrically isolated (myelinated) from the surrounding electrolyte solution. The myelin sheath presents a crucial evolutionary innovation. In a process called saltatory conduction, the neural impulse propagates from node to node more rapidly than it propagates in unmyelinated axons of equal diameter [1,2]. Myelination not only helped nature to increase the signal propagation speed, but also to drastically reduce the metabolic cost of neural computation. Indeed, with a single neural impulse (of the order of 1 ms), each sodium channel transfers up to 10^4 sodium ions into the cell, which then should be pumped back to restore the appropriate steady-state electrochemical potential. To transfer three sodium ions, the corresponding Na-K pump hydrolyzes one ATP molecule [2], which thus yields an estimate of about 3×10^3 ATP molecules per ion channel per neural spike. A too large number of channels imposes an extremely high metabolic load (the brain of the reader is just now consuming about 10% of the body's metabolic budget, which, per one kilogram of mass, is more than the muscles use when active). More elaborate estimates confirm that even a small cortical cell needs, in a long run, at least 10^7 ATP molecules per one neural spike [3,4].

In myelinated neurons, yet another problem emerges: there is a threshold present for the electrical coupling between the nodes of Ranvier. Deterministic cable equation models predict that if the internodal distance is too large, the coupling becomes too small and the signal propagation consequently fails [2]. However, due to a finite number of channels (of the order of 10^4), intrinsic noise is inevitably present in the nodes of Ranvier [5]. The deterministic models can only mimic the behavior of a very large number of ion channels possessing a negligible intrinsic noise intensity; in contrast, real neurons tend to minimize the number of ion channels because of energetic costs. On the other hand, too few channels may trigger random, parasitic spikes or induce spike suppression by strong fluctuations, making the signal transmission too noisy and thus unreliable. The questions we investigate in this paper within a simplified stochastic model

of signal transmission in a myelinated neuron are as follows: can channel noise soften the propagation threshold and facilitate the signal propagation which would not occur in the deterministic case? Does an optimum size of the channel cluster exist, which in turn yields a most efficient, noise-assisted propagation?

The statement of this objective shares features similar in spirit to noise supported wave propagation in subexcitable media (see Ref. [6] and references therein) and noise in excitable spatiotemporal systems (see Ref. [7]). The influence of intrinsic noise on membrane dynamics was studied in the context of intrinsic stochastic resonance (see in Refs. [8,9]) and synchronization of ion channel clusters [10]. A new aspect emerging from the present study is a possible interpretation of the neural spike transmission as a delayed synchronization phenomenon occurring in the chain of active elements [11–13].

II. MODEL

A. Compartment modeling for myelinated axons

As an archetypical model for signal transmission along a myelinated axon of a neuronal cell, we consider a compartmental stochastic Hodgkin-Huxley model (see Secs. II B and II C). In contrast to unmyelinated axons, where ion channels are homogeneously distributed within the membrane, the myelinated axon consists of alternating sections where the ion channels are densely accumulated (nodes of Ranvier) and regions with very low ion channel density, encased in multiple layers of a highly resistive lipid sheath called myelin. The nodes of Ranvier play the role of *active* compartments in our model, while the electrically neutral myelinated segments constitute *passive* compartments (see Fig. 1). The typical internodal distance L is about 1–2 mm, while the length λ of the nodes of Ranvier is in the micrometer range [1].

The generalization of the original Hodgkin-Huxley model is related to the influence of the channel noise, which results from the randomness of the ion channel gating. The membrane potential at each particular node of Ranvier is assumed to be constant across the whole node area and is characterized by V_i , $i=0, 1, 2, \dots, N-1$, where N is the total number of nodes [1,2].

Supposing total electrical neutrality of the *passive* re-

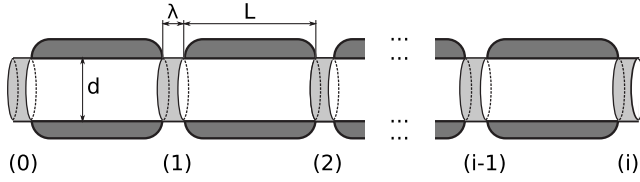


FIG. 1. Sketch of a myelinated axon: The axonal cell membrane in the nodes of Ranvier (depicted in light gray) contains a high ion channel concentration. The remaining segments are wrapped in the myelin sheath (dark gray). Spike propagation along the axon occurs in a saltatory manner.

regions, the electrical properties of a myelinated axon are modeled by a linear chain of diffusively coupled active elements. The dynamics of the membrane potential is given by

$$C \frac{d}{dt} V_i = I_{i,\text{ionic}}(V_i, t) + I_{i,\text{ext}}(t) + I_{i,\text{inter}},$$

$$\text{for } i = 0, 1, 2, \dots, N-1, \quad (1)$$

where C denotes the axonal membrane capacity per unit area. $I_{i,\text{ionic}}(V_i, t)$ is the ionic membrane current (per unit area) within the i th node of Ranvier. $I_{i,\text{ionic}}(V_i, t)$ depends on time t and on the membrane potential V_i in the specific node i only, and is described by a neuronal membrane model which we subsequently treat within a coupled stochastic Hodgkin-Huxley setup. $I_{i,\text{ext}}(t)$ describes an external current per unit area applied on the i th node. In our setup we apply the stimulus—i.e., a constant current—on the first node only, bringing it into a dynamical regime of periodic firing [14]. If the coupling between nodes is sufficiently strong, the action potentials may start propagating along the axon. The coupling to the next-neighboring nodes of Ranvier is achieved by internodal currents (per unit area) $I_{i,\text{inter}}$ given as

$$I_{i,\text{inter}} = \begin{cases} \kappa(V_{i+1} - V_i) & \text{for } i = 0, \\ \kappa(V_{i-1} - V_i) & \text{for } i = N-1, \\ \kappa(V_{i-1} - 2V_i + V_{i+1}) & \text{elsewhere.} \end{cases} \quad (2)$$

The coupling parameter κ depends, among other things, on the length L of the internodal *passive* segment of the axon as well as on the resistivity of the extracellular and intracellular medium and serves as a control parameter in our studies [1]. It depends also on the ratio of the node's diameter d and its length λ . Typically, the node's diameter is two orders of magnitude smaller than its length [2].

Note that Eq. (1) just presents the Kirchhoff law for an electrical circuit made of membrane capacitors, variable nonlinear membrane conductances, and internodal conductances κ .

B. Hodgkin-Huxley modeling

According to the standard Hodgkin-Huxley model [15] the ionic membrane current reads

$$I_i(V_i) = -G_K(n_i)(V_i - E_K) - G_{\text{Na}}(m_i, h_i)(V_i - E_{\text{Na}}) - G_L(V_i - E_L), \quad (3)$$

with the potassium and sodium conductances per unit area given by

$$G_K(n_i) = g_K^{\text{max}} n_i^4, \quad G_{\text{Na}}(m_i, h_i) = g_{\text{Na}}^{\text{max}} m_i^3 h_i. \quad (4)$$

In Eq. (3), V_i denotes the membrane potential at the i th node of Ranvier. Furthermore, E_{Na} , E_K , and E_L are the reversal potentials for the potassium, sodium, and leakage currents, correspondingly. The leakage conductance per unit area, G_L , is assumed to be constant. The parameters g_K^{max} and $g_{\text{Na}}^{\text{max}}$ denote the maximum potassium and sodium conductances per unit area, when all ion channels within the corresponding node are open. The values of these parameters are collected in Table I [16]. Note that in the nodal membrane the conductances of *open* ion channels are supposed to be Ohmic-like; i.e., the nonlinearity derives from their gating behavior only. Moreover, formulating Eqs. (3) and (4), we implicitly assumed for simplicity that the different axonal nodes are kinetically identical: i.e., the number of sodium and potassium ion channels is constant for each node. As a consequence, the maximum potassium and sodium conductances are identical constants for every node of Ranvier.

The gating variables n_i , m_i , and h_i [cf. Eqs. (3) and (4)] describe the probabilities of opening the gates of the specific ion channels in the i th node upon the action of activation and inactivation particles. h is the probability that the one inactivation particle has not caused the Na gate to close. m is the probability that one of the three required activation particles has contributed to the activation of the Na gate. Similarly, n is the probability of the K gate activation by one of the four required activation particles. Assuming gate independence, the factors n_i^4 and $m_i^3 h_i$ are the mean portions of the open ion channels within a membrane patch. The dynamics of the gating variables are determined by voltage-dependent opening and closing rates $\alpha_x(V)$ and $\beta_x(V)$ ($x=m, h, n$) taken at $T = 6.3$ °C. They depend on the local membrane potential V and read (with numbers given in units of [mV]) [15,17]

$$\alpha_m(V) = 0.1 \frac{V + 40}{1 - \exp\{-(V + 40)/10\}}, \quad (5a)$$

$$\beta_m(V) = 4 \exp\{-(V + 65)/18\}, \quad (5b)$$

$$\alpha_h(V) = 0.07 \exp\{-(V + 65)/20\}, \quad (5c)$$

$$\beta_h(V) = \frac{1}{1 + \exp\{-(V + 35)/10\}}, \quad (5d)$$

$$\alpha_n(V) = 0.01 \frac{V + 55}{1 - \exp\{-(V + 55)/10\}}, \quad (5e)$$

$$\beta_n(V) = 0.125 \exp\{-(V + 65)/80\}. \quad (5f)$$

The dynamics of the mean fractions of open gates reduces in the standard Hodgkin-Huxley model to relaxation dynamics:

TABLE I. Model and simulation parameters.

Stochastic Hodgkin-Huxley model				
Membrane capacitance per unit area	C	=	1	$\mu\text{F}/\text{cm}^2$
Reversal potential for Na current	E_{Na}	=	50	mV
Reversal potential for K current	E_{K}	=	-77	mV
Reversal potential for leakage current	E_{L}	=	-54.4	mV
Leakage conductance per unit area	G_{L}	=	0.25	mS/cm^2
Maximum Na conductance per unit area	$g_{\text{Na}}^{\text{max}}$	=	120	mS/cm^2
Maximum K conductance per unit area	$g_{\text{K}}^{\text{max}}$	=	36	mS/cm^2
Node area	\mathcal{A}	varying		$[\mu\text{m}^2]$
Na channel density	ρ_{Na}	=	60	μm^{-2}
K channel density	ρ_{K}	=	18	μm^{-2}
Number of Na channels	N_{Na}	=	$\rho_{\text{Na}}\mathcal{A}$	
Number of K channels	N_{K}	=	$\rho_{\text{K}}\mathcal{A}$	
Axonal chain model				
Internodal conductance per unit area	κ	=	0.065	mS/cm^2
Number of nodes	N	=	10	
Simulation parameters				
External current per unit area, node 0	$I_{0,\text{ext}}$	=	12	$\mu\text{A}/\text{cm}^2$
External current per unit area, other nodes	$I_{i=1,\dots,N-1,\text{ext}}$	=	0	$\mu\text{A}/\text{cm}^2$
Simulation time	T	=	3×10^5	ms
Simulation time step	dt	=	0.002	ms
Initial values for each node ($i=0, \dots, N$)				
Voltage	V_i	=	-59.9	mV
Inactivation probability for the Na gate	h_i	=	0.414	
Activation probability for the Na gate	m_i	=	0.095	
Activation probability for the K gate.	n_i	=	0.398	

$$\frac{d}{dt}x_i = \alpha_x(V_i)(1-x_i) - \beta_x(V_i)x_i, \quad x = m, h, n. \quad (6)$$

Such an approximation is valid for very large numbers of ion channels and whenever fluctuations around their mean values are negligible.

C. Stochastic generalization of the Hodgkin-Huxley model

Because the size of the nodal membrane is finite, there necessarily occur fluctuations of the number of open ion channels. This is due to the fact that the ion channel gating between open and closed state is random. Accordingly, for finite-size membrane patches like the considered nodes of Ranvier, there are fluctuations of the membrane conductance which give rise to *spontaneous* action potentials [1,8,9,18–20] and references therein.

The number of open gates undergoes a birth-and-death-like process. The corresponding master equation can readily be written down. The use of a Kramers-Moyal expansion in

that equation results in a corresponding Fokker-Planck equation which provides a diffusion approximation to the discrete dynamics [19,20]. The corresponding multiplicative noise Langevin equations [21] then read

$$\frac{d}{dt}x_i = \alpha_x(V_i)(1-x_i) - \beta_x(V_i)x_i + \xi_{i,x}(t), \quad (7a)$$

with $x = m, h, n$. Here, $\xi_{i,x}(t)$ are independent Gaussian white-noise sources of vanishing mean and vanishing cross correlations. For an excitable node with the nodal membrane size \mathcal{A} the nonvanishing noise correlations take the following form:

$$\langle \xi_{i,m}(t) \xi_{i,m}(t') \rangle = \frac{1}{\mathcal{A}\rho_{\text{Na}}} [\alpha_m(V_i)(1-m_i) + \beta_m(V_i)m_i] \delta(t-t'), \quad (7b)$$

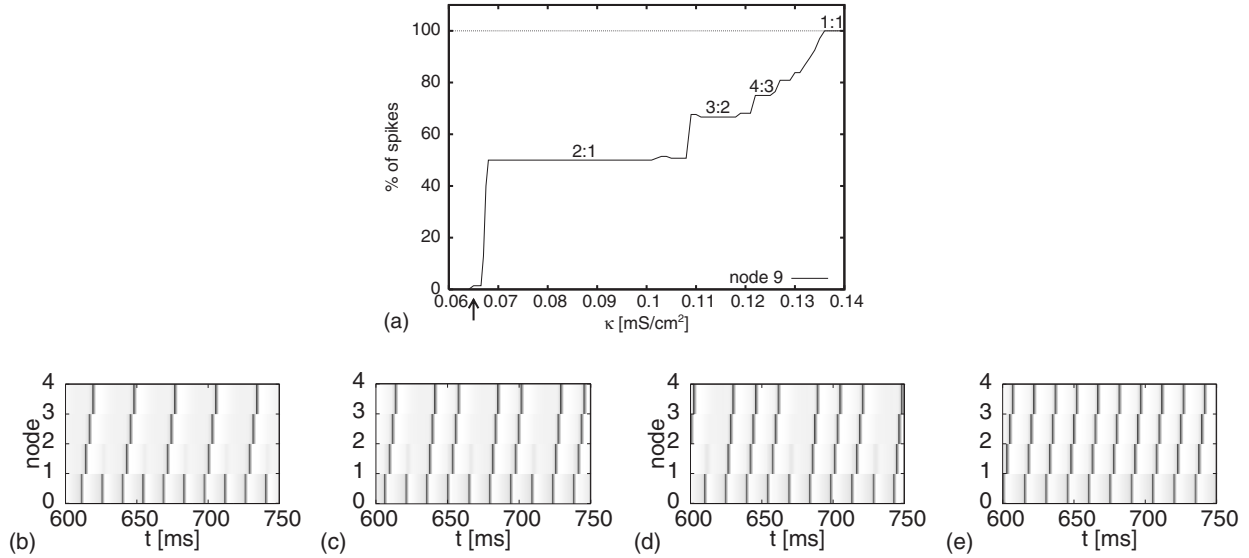


FIG. 2. Deterministic spike propagation in a myelinated axon containing $N=10$ Ranvier nodes (no channel noise): (a) The ratio of spikes generated in the node 0 during an interval of 1000 ms which propagate up to the node 9 (solid line), as a function of the value of the internodal coupling strength (i.e., the conductance) κ . The arrow indicates the subthreshold value of $\kappa=0.065$ mS/cm² chosen for further simulations of the influence of channel noise on spike propagation. The stepwise shape of the graph depicts the different transmission patterns [see (b) 2:1, (c) 3:2, (d) 4:3, and (e) 1:1]. For example, for the ratio of 2:1, every second spike which is generated at $n=0$ propagates. (Small irregularities in step levels occur as a result of a finite counting statistics of propagating spikes.)

$$\langle \xi_{i,h}(t) \xi_{i,h}(t') \rangle = \frac{1}{\mathcal{A} \rho_{Na}} [\alpha_h(V_i)(1 - h_i) + \beta_h(V_i)h_i] \delta(t - t'), \tag{7c}$$

$$\langle \xi_{i,n}(t) \xi_{i,n}(t') \rangle = \frac{1}{\mathcal{A} \rho_K} [\alpha_n(V_i)(1 - n_i) + \beta_n(V_i)n_i] \delta(t - t'), \tag{7d}$$

with the ion channel densities being ρ_{Na} and ρ_K (see Table I). The stochastic equation (7a) replaces Eq. (6) [22]. Remarkably, the nodal membrane size \mathcal{A} , which is the same for all nodes, solely influences the intrinsic noise strength. Note that the correlations of the stochastic forces in these Langevin equations contain the corresponding state-dependent variables and, being an approximation to the full master equation dynamics, thus should be interpreted in the Itô sense [23].

III. OPTIMIZATION OF THE SIGNAL PROPAGATION

We next study the model of a myelinated axon in which one node of Ranvier is continuously excited to spontaneous spiking by an external suprathreshold current, whereas other nodes are initially in the resting state and the internodal conductance κ is too low for the spikes to propagate to the neighboring nodes in the deterministic model (notice the arrow in Fig. 2). The fluctuations of the potential caused by the randomly opening and closing channels can be large enough to help the spike to overcome the large internodal resistance and to make the saltatory conduction between nodes possible.

A. Deterministic limit

We start out with the deterministic situation using a finite number of Ranvier nodes; i.e., the channel noise level is set to zero, which is formally achieved in the limit $\mathcal{A} \rightarrow \infty$. In order to provide some insightful explanation of the dependence of saltatory spike propagation on the coupling parameter, we numerically integrated the dynamical system [see Eqs. (1)–(6)] with the parameters given in Table I. In order to achieve equilibration along the whole chain we do not apply the constant current on the first node $I_{0,ext}$ from the beginning. Instead, we use the following protocol: (i) we initially allow for equilibration of every individual node by integrating over 100 ms with $\kappa=0$; (ii) in a second step, we switch on the coupling; (iii) finally, after integrating over 150 ms—i.e., under stationary conditions—we apply a constant current stimulus of $I_{0,ext}=12 \mu\text{A}/\text{cm}^2$ on the first node only. Due to the suprathreshold stimulus [8] on the first node, the dynamics of the membrane potential of the initial node V_0 exhibits a limit cycle, resulting in the periodic generation of action potentials. The numerically obtained spike trains V_i for $i=0, \dots, 9$ allow for studying the propagation of action potentials along the linearly coupled chain. Using a threshold value of $V_{th}=20$ mV enables the detection of an action potential (also called spike or firing event) in the particular spike train of the individual nodes. Since we are interested in the successful transmission along the whole chain, the spiking at the terminal node is analyzed and the number of spikes at the terminal node is related to the number of initiated spikes at the initial node. This defines the transmission reliability.

For the chosen coupling strength κ , the excitation propagates along the chain of given $N=10$ nodes of Ranvier. This particular choice of the number of nodes is somewhat arbitrary.

trary, although physiologically realistic. Note also that these obtained results are robust and are typical for larger node numbers as well (not shown). Obviously, for too small coupling parameters no excitation proceeds to the neighboring node “1” and, at the end, will not reach the terminal node “9.” In this case, we observe that spike propagation fails. In the opposite limit—i.e., for large coupling constants κ —each action potential travels along the chain and arrives at the terminal node “9.” Then the spike transmission efficiency of 100% is achieved. In this situation, the dynamics of the terminal node is synchronized with a delay with the initial node—i.e., $V_9(t) = V_0(t - \tau)$, where the delay time τ accounts for the finite propagation speed. Most interestingly, however, there occurs no sharp transition between those two regimes of 0% and 100% signal transmission (see Fig. 2). For $\kappa_{c1} = 0.0665$ mS/cm² and $\kappa_{c2} = 0.1360$ mS/cm², there is an intermediate regime $\kappa_{c1} < \kappa < \kappa_{c2}$ where discrete transmission patterns $k:l$ occur. Here, k is the number of spikes generated at the initial node, while l corresponds to the number of spikes transmitted to the final node. In principle, the coupling parameter κ could be tuned in such a way that several different rational transmission patterns $k:l$ are attained. This manifests as generalized, delayed synchronization.

Note that a similar effect shows up when one drives the Hodgkin-Huxley system (i.e., a single node) with an acinusoidal signal, where the ratio of spiking events to driving periods exhibits a rational number [24].

B. Influence of channel noise

Next, we investigate how the nodal membrane size \mathcal{A} , determining the channel noise intensity, influences the propagation of spikes along the axon. Towards this objective we numerically integrated the linearly coupled chain model with the nodes treated by the stochastic Hodgkin-Huxley model [cf. Eqs. (1)–(5) and Eqs. (7a)–(7d)].

Following the same protocol as for the deterministic case, we computed the probability for a generated spike in the initial node to be transduced to the terminal node. In our example the axon consists again of ten nodes. For the coupling parameter—i.e., the internodal conductance—we chose a subthreshold value of $\kappa = 0.065$ mS/cm²—i.e., below the critical value κ_{c1} for a deterministic spike propagation along the axon (see Fig. 2). It turns out that for coupling parameters slightly smaller than the critical value κ_{c1} the influence of the channel noise is most striking. Due to the channel noise, we observe spike propagation even for the *subthreshold* coupling—i.e., for $\kappa < \kappa_{c1}$. The intrinsic noise weakens the strict threshold, and even for subthreshold values of the coupling parameter, there is a nonvanishing probability for spike propagation. In Fig. 3 the spike train for three different nodes is shown for $\kappa = 0.065$ mS/cm² and $\mathcal{A} = 10^4$ μm^2 —i.e., for an intermediate intrinsic noise level. The channel noise facilitates the propagation of action potentials along the axonal chain.

Figure 4 depicts cases of spike propagation in the presence of noise of different intensities for the chosen subthreshold coupling parameter κ . Apart from the noise-facilitated spike propagation one can identify another

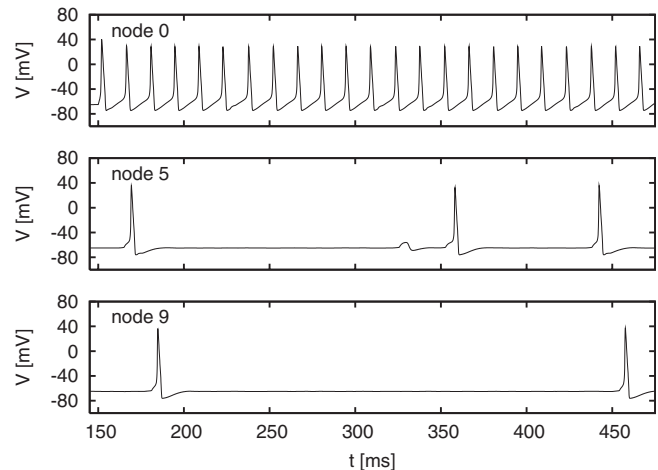


FIG. 3. The simulated firing events vs time [cf. Eqs. (1)–(5) and (7a)–(7d)] of the noisy membrane potentials at three different nodes are depicted for $\kappa = 0.065$ mS/cm² and the nodal area $\mathcal{A} = 10^4$ μm^2 . The constant-current stimulus $I_{0,\text{ex}}$ keeps the initial node “0” periodically firing. Noise-assisted spike propagation occurs for some spikes, and other spikes do not reach the terminal node “9.”

particular phenomenon: The failure of spike propagation due to a large channel noise level. For rather strong intrinsic noise (for small nodal membrane sizes \mathcal{A} , yielding small numbers of ion channels) the spike initiated at the first node more likely propagates to the next nodes. However, it is also likely that the spike collides with a particularly large fluctuation and thus becomes deleted. Tracking the behavior of a given node, one observes the skipping of some firing events [25] (see Fig. 3). The propagation distance is then quite short, and the excitations rarely arrive at the terminal node [see Fig. 4(a)]. Note also that for a high level of channel noise spontaneous spikes can occur at any node. These *parasitic* spikes are not triggered by a preceding spike in the neighboring nodes. Therefore, they deteriorate the information transfer along the axon and are not considered for the spiking statistics at the terminal node.

Too weak noise (i.e., a large number of channels) does not allow for effective spike transmission to neighboring nodes. Only the very first excitation is transmitted over a larger number of nodes, while the propagation of the successive action potentials is rarely facilitated by noise [see Fig. 4(c)]. This specific enabling of propagation of the first spike only is due to the initial setup of the problem (initial conditions).

For an intermediate channel noise intensity, however, the propagation distance is the longest, although spikes propagate less frequently than in the presence of an intensive noise [see Fig. 4(b)]. Overall, one may expect that there is an optimum dose of internal noise for which the spike propagation along an axon is most probable. To validate this assertion, we determined the probability for an excitation stimulated in the initial node to arrive at the terminal node “9” in our case. The fraction of spikes arriving at a specific node depends on both the distance which has to be covered and the noise level. With increasing distance—i.e., the node number—this fraction declines monotonically [cf. Fig. 5(a)]. The decay depends on the channel noise level—i.e., the nodal membrane size \mathcal{A} . There is an intermediate noise level for which

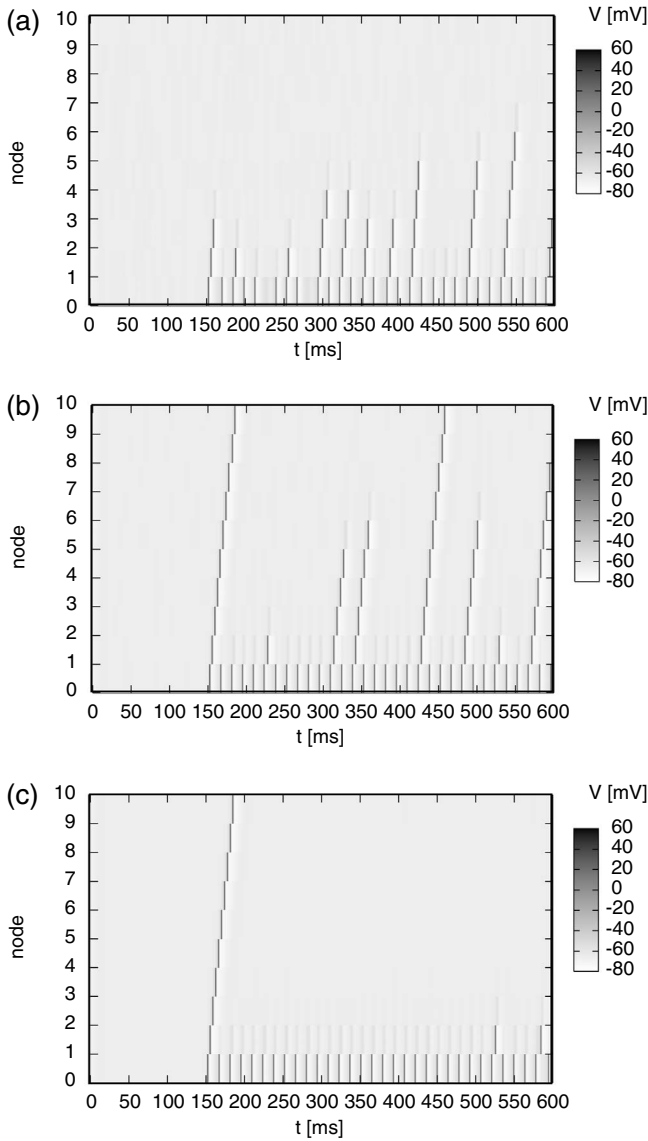


FIG. 4. Noisy spike propagation for a myelinated neuron with ten Ranvier nodes. Single realizations of noise-assisted spike propagation for varying nodal membrane size \mathcal{A} . (a) $\mathcal{A}=250 \mu\text{m}^2$: Strong channel noise inhibits strongly spike propagation so that propagation occurs only over a short distance. (b) $\mathcal{A}=10^4 \mu\text{m}^2$: An intermediate noise allows for the propagation over the longest distance. (c) $\mathcal{A}=5 \times 10^4 \mu\text{m}^2$: Weak channel noise only rarely allows one to overcome the internodal resistance.

the decline is slowest. As a result, there exists an optimum dose of internal noise (in our example for the nodal membrane size near $\mathcal{A} \approx 3800 \mu\text{m}^2$) at which the signal transmission to the terminal node is most effective; i.e., the ratio of transmitted spikes assumes a maximum [cf. Fig. 5(b)]. We emphasize that the occurrence of the optimal dose of intrinsic noise is robust under a change of the total number of nodes (not shown). Note that the observed maximum corresponds to a nodal number of sodium ion channels of $N_{\text{Na}} = 2.28 \times 10^5$, which corroborates with the physiological range of the number found for sodium ion channels in a node of Ranvier (experimental studies report $N_{\text{Na}} \approx 10^5$) [26,27].

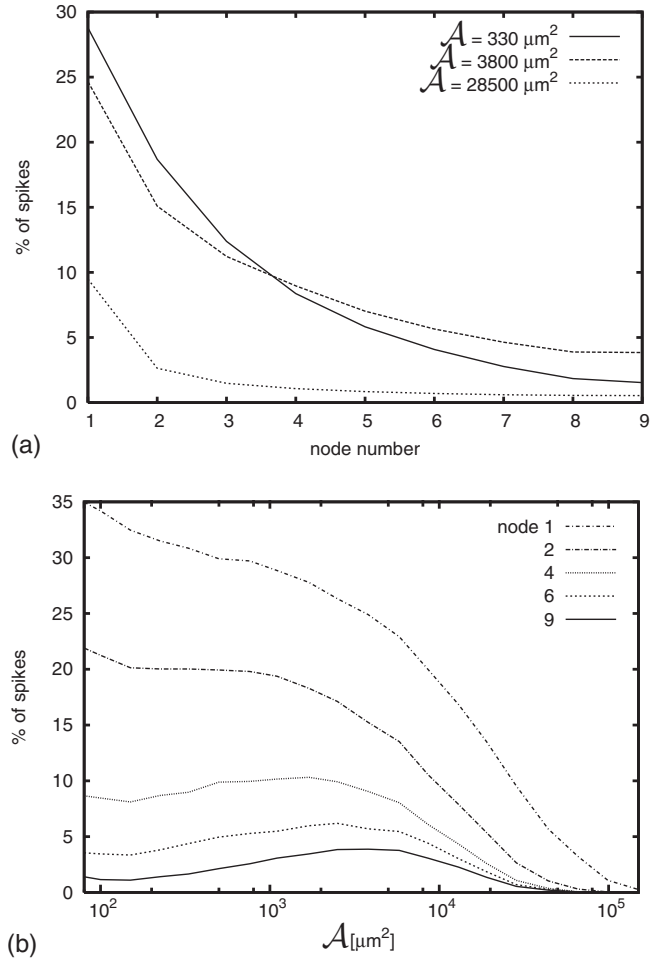


FIG. 5. Noise-assisted spike propagation for spikes initiated in the initial node (“0”) out of ten nodes of a linearly coupled chain: (a) The numerically obtained percentage of spike arrivals at the particular nodes and (b) its dependence on the nodal membrane size \mathcal{A} . The chosen coupling strength $\kappa=0.065 \text{ mS/cm}^2$ is subthreshold. There occurs an optimum noise intensity (corresponding to a nodal membrane size $\mathcal{A} \approx 3800 \mu\text{m}^2$) at which the signal transmission along the whole chain is most efficient.

IV. CONCLUSIONS

The optimization of the signal propagation along a myelinated axon of a finite size occurs as the result of the competition between the constructive and destructive role of channel noise occurring in the nodes of Ranvier. On the one hand, when the number of channels in the node is very small, the strong fluctuations of the activation potential facilitate a spike propagation among nodes, which otherwise does not occur in the absence of channel noise. On the other hand, at a high level of channel noise spikes cannot travel over a long distance because it is likely that a spike soon collides with another noise-induced spike, leading to their mutual annihilation, or the noise can also suppress spike generation. If the number of channels in nodes is large, the fluctuations are too weak for a spike to overcome the internodal resistance and subsequently to propagate. For a certain intermediate number of channels in the node of Ranvier, however, the intrinsic noise is sufficiently strong to induce the saltatory conduction

while being still sufficiently weak not to deteriorate the spiking behavior. An optimal nodal membrane size can be identified, for which the signal becomes most efficiently transmitted over a certain axonal distance. Moreover, the corresponding number of sodium ion channels corresponds to actual physiological values. This feature is quite in spirit of the stochastic resonance phenomenon [28,29] with an intrinsic noise source [8,9]. One may therefore speculate whether nature adopted this optimization method to balance

the signal transmission efficiency and the metabolic cost.

ACKNOWLEDGMENTS

This work has been supported by the Volkswagen Foundation (Project No. I/80424), the collaborative research center of the DFG via SFB-486, Project No. A-10, and the German Excellence Initiative via the “Nanosystems Initiative Munich” (NIM).

-
- [1] C. Koch, *Biophysics of Computation, Information Processing in Single Neurons* (Oxford University Press, New York, 1999).
- [2] J. Keener and J. Sneyd, *Mathematical Physiology* (Springer, New York, 2001).
- [3] S. B. Laughlin, R. R. de Ruyter van Steveninck, and J. C. Anderson, *Nat. Neurosci.* **1**, 36 (1998); S. B. Laughlin and T. J. Sejnowski, *Science* **301**, 1870 (2003).
- [4] S. M. Bezrukov and L. B. Kish, *Smart Mater. Struct.* **11**, 800 (2002).
- [5] H. Lecar and R. Nossal, *Biophys. J.* **11**, 1048 (1971); **11**, 1068 (1971).
- [6] F. Sagués, J. M. Sancho, and J. García-Ojalvo, *Rev. Mod. Phys.* **79**, 829 (2007).
- [7] B. Lindner, J. García-Ojalvo, A. Neiman, and L. Schimansky-Geier, *Phys. Rep.* **392**, 321 (2004).
- [8] G. Schmid, I. Goychuk, and P. Hänggi, *Europhys. Lett.* **56**, 22 (2001).
- [9] P. Jung and J. W. Shuai, *Europhys. Lett.* **56**, 29 (2001).
- [10] S. Zeng, Y. Tang, and P. Jung, *Phys. Rev. E* **76**, 011905 (2007); S. Zeng and P. Jung, *Phys. Rev. E* **71**, 011910 (2005).
- [11] D. Hennig and L. Schimansky-Geier, *Physica A* **387**, 967 (2008).
- [12] D. Hennig and L. Schimansky-Geier, *Phys. Rev. E* **76**, 026208 (2007).
- [13] E. Glatt, M. Gassel, and F. Kaiser, *Europhys. Lett.* **81**, 40004 (2008).
- [14] E. M. Izhikevich, *Int. J. Bifurcation Chaos Appl. Sci. Eng.* **10**, 1171 (2000).
- [15] A. L. Hodgkin and A. F. Huxley, *J. Physiol. (London)* **117**, 500 (1952).
- [16] It is worth noticing that in our model study we use parameters for the squid giant axon. In realistic nodes of Ranvier, the sodium ion channel density is larger at least by a factor of 10 than that of the potassium ion channels. A physiologically more realistic model is left for a separate study.
- [17] I. Goychuk and P. Hänggi, *Proc. Natl. Acad. Sci. U.S.A.* **99**, 3552 (2002).
- [18] C. C. Chow and J. A. White, *Biophys. J.* **71**, 3013 (1996).
- [19] H. C. Tuckwell, *J. Theor. Biol.* **127**, 427 (1987).
- [20] R. F. Fox and Y. N. Lu, *Phys. Rev. E* **49**, 3421 (1994).
- [21] P. Hänggi and H. Thomas, *Phys. Rep.* **88**, 207 (1982); see Sec. 6.2.
- [22] G. Schmid, I. Goychuk, and P. Hänggi, *Phys. Biol.* **3**, 248 (2006).
- [23] P. Hänggi and H. Thomas, *Phys. Rep.* **88**, 207 (1982); see Sec. 2.4.
- [24] K. Aihara, G. Matsumoto, and Y. Ikegaya, *J. Theor. Biol.* **109**, 249 (1984).
- [25] G. Schmid, I. Goychuk, and P. Hänggi, *Physica A* **325**, 165 (2003).
- [26] F. J. Sigworth, *J. Physiol. (London)* **307**, 97 (1980).
- [27] F. Conti and E. Wanke, *Q. Rev. Biophys.* **8**, 451–506 (1975).
- [28] L. Gammaitoni, P. Hänggi, P. Jung, and F. Marchesoni, *Rev. Mod. Phys.* **70**, 223 (1998).
- [29] P. Hänggi, *ChemPhysChem* **3**, 285 (2002).